Supporting Information

Enzymatically hydrolyzed oligosaccharide fingerprinting using nanopipettes at the single-molecule level

Qi-Yun Lu[‡a], Hui Ma[‡*b], Shi-Guo Chen[*a]

[a] College of Biosystems Engineering and Food Science, National-Local Joint Engineering Laboratory of Intelligent Food Technology and Equipment, Zhejiang Key Laboratory for Agro-Food Processing, Zhejiang Engineering Laboratory of Food Technology and Equipment, Zhejiang University, Hangzhou 310058, P.R. China

[b] School of Chemistry and Chemical Engineering, Zhejiang Sci-Tech University, Hangzhou, 310038, P.R. China

[‡] These authors contributed equally to this work.

Email: chenshiguo210@163.com; huima@zstu.edu.cn

Table of Contents

Supplementary Methods

Materials

Polygalacturonic Acid (Galacturonic acid ≥ 90%, enzymatic, $M_w \approx 150$ kDa) were purchased from Sigma-Aldrich (Shanghai, China). Endo-Polygalacturonase (E-PGALPC) was obtained from Megazyme (Ireland). All Monosaccharide standards (≥ 97%), Acetonitrile (≥ 99.9%) and Formic acid (≥ 98%) were from Sigma-Aldrich (Shanghai, China). Sodium hydroxide (≥ 96%), Hydrochloric acid (36-38%), Sulphuric acid (95-98%), Sodium acetate (≥ 99%), Phenol (≥ 99%) were from HuShi (China). Ammonium bicarbonate (≥ 98%), Sodium chloride (≥ 99.5%), Sodium borohydride (≥ 98%) and Potassium bromide (≥ 99.5%) were from Aladdin ((Shanghai, China). Deuterium oxide (99.8% D) was from Energy (China). All the freeze-drying process were performed by an Alpha 1-4 LD plus (Christ, Germany). The pH of the solutions was measured by a PE28-standard pH meter (Mettle-Toledo, Zurich, Switzerland). Quartz capillaries (length =7.5 cm, o.d. = 1.0 mm, i.d. = 0.5 mm, QF 100-50-10) were purchased from Sutter Instrument Co. (California, USA). The nanopipettes were characterized by Field emission transmission electron microscopy (TEM, Tecnai F20, FEI, Czech Republic). All solutions were prepared by deionized water with a resistance of 18.2 MΩ·cm at 23 ± 2°C from a Milli-Qsystem (Massachusetts, USA).

Preparation of galacturonic acid oligosaccharides

Galacturonic acid oligosaccharide standards were prepared by commercially available Polygalacturonic Acid via enzymatic degradation. A specific Endo-Polygalacturonase was used to cleave the α-1,4 glycosidic bonds, with the enzymatic conditions adjusted to produce oligosaccharides of varying degrees of polymerization.[1] Prior to this, a demethylesterification reaction was necessary to eliminate the steric hindrance from the methyl ester at C6 of galacturonate.[2] 1 g of standard pectin was dissolved in 50 mL of deionized water, to which 50 mL of 0.1 M NaOH containing 40 mM of $NaBH_4$ was added. The reaction was performed on ice to inhibit the cleavage of principal chain and was neutralized to pH4.5 with hydrochloric acid after fully demethylesterified for 30 minutes. The demethylesterified pectin was then dialyzed in 10 kDa for 2-3 days with continuous replacement of deionized water to completely remove salts and methanol. The pectin was freeze-dried and subjected to Fourier-transform infrared spectroscopy to ensure complete removal of methyl ester groups. The demethylesterified pectin was then dissolved in a 0.1 M sodium acetate solution at pH5.5 to make a 2 mg/mL solution, and digested with 0.1 mU/mg of the Endo-Polygalacturonase at 50°C. The degree of enzymatic hydrolysis was monitored using Gel Permeation Chromatography, and the enzyme was inactivated by heating at 100°C for 10 minutes, and freeze-dried for 48h.

Purification of galacturonic acid oligosaccharides

Galacturonic acid oligosaccharides were further purified by gel filtration on a Superdex peptide 30 column (2.6 × 100 cm), followed by separation on an XAmide column (5 μm, 10 × 150 mm, Acchrom, China). Briefly, 100 mg of freeze-dried enzymatic hydrolysate was dissolved in 10 mL of deionized water and loaded onto Superdex peptide 30. Elution was performed at room temperature with 0.3 M NH_4HCO_3 at a flow rate of 0.5 mL/min. The eluate was collected automatically at 10 min per tube. A 40 μL aliquot from every fifth tube was analyzed by the phenol–sulfuric acid method, and the sugar-containing fractions were pooled and freeze-dried.

The crude oligosaccharide fractions were then redissolved in deionized water, filtered through a 0.22 μm membrane, and further purified by preparative hydrophilic interaction liquid chromatography (HILIC) using an XAmide column coupled with an evaporative light-scattering detector (Unimicrotech, China) at room temperature. This purification step was repeated 3–4 times. Mobile phase A consisted of 20% acetonitrile

containing 0.2% (v/v) formic acid, and mobile phase B consisted of 80% acetonitrile containing 0.2% (v/v) formic acid. Gradient elution was performed at a flow rate of 5 mL/min as follows: 0–35 min, 100%–70% B; 35–50 min, 70%–20% B; 50–55 min, 20% B; 55–56 min, 20%–100% B; and 56–60 min, 100% B. A two-way valve was used to reduce the flow rate entering the detector to 1 mL/min. Individual chromatographic peaks corresponding to purified oligosaccharides were collected separately and freeze-dried.

SEC-MALLS Analysis

The Molecular weight (M_w), number-average molecular weight (M_n), polydispersity (M_w/M_n) were estimated using High-performance size exclusion chromatography (SEC) (SB-806 HQ and SB-804 HQ column, 7.8 x 300 nm, Shodex, Japan) coupled with multi-angle laser light scattering (DAWN HELEOS II, Wyatt Technology, USA) and refractive index (SEC-MALLS-RI). 2 mg of polysaccharides was dispersed in 1 mL deionized water and filtered through a 0.22 μm membrane. 50 μL sample solution was injected into the chromatographic system and passed through the column with 0.15 M sodium chloride solution at a 0.5 mL/min flow rate under 40°C. The molar mass was calculated with a dn/dc value of 0.1380 mL/g (a universal value for the carbohydrate polymer). Data was analyzed on ASTRA software 7.3.2 (Waters, USA).

Monosaccharide composition analysis

The monosaccharide composition was determined by High-performance anion-exchange chromatography with pulsed amperometry detection (HPAEC-PAD). 1 mg of polysaccharide was hydrolyzed in 1 mL of 2 M trifluoroacetic acid (TFA) at 110°C for 6 hours. Methanol was then added under nitrogen to help completely evaporate the TFA. Next the sample was dispersed in 5 mL distilled water, and filtered through a 0.22 μm membrane. 25 μL of each sample solution was injected into an ICS-5000 system (Thermo Fisher, USA) combined with a Carbopac-PA10 analytical column (4 x 250 mm, Thermo Fisher, USA) and an electrochemical detector (AgCl reference electrode). The whole process used isocratic elution at a flow rate of 1 mL/min: the column was washed with 24 mM NaOH for 15 mins, followed with NaOAc solution (100 mM) containing 18 mM NaOH for the next 35 mins, and the column temperature was 35°C. The standards of ten monosaccharides mixtures in different concentrations (400 μM, 200 μM, 100 μM, 50 μM, 25 μM) were also detected using the same method and calculated the monosaccharide composition of each sample.

Fourier-transform infrared (FT-IR) spectroscopy

The fourier-transform infrared (FT-IR) spectra of polysaccharides were obtained by A Nicolet iN10 instrument (Thermo Fisher Scientific, USA). Approximately 1 mg of polysaccharide was mixed and ground with 200 mg of KBr into small pellets, turning to absorbance measuring after the blank background was removed. The scanning frequency range was 4000−400 cm^{-1}. The absorption peaks at about 1740 and 1630 cm^{-1} were attributed to the methylesterificated carboxyl group (COO−R) and unmethylesterificated carboxyl groups (COO^-). Degrees of methylesterification of pectin were estimated through the ratio of the peak area at 1740 cm^{-1} over the sum of the peak areas of 1740 and 1630 cm^{-1} which was based on Eq. (1).[4]

$DM\% = A_{1740} / (A_{1740} + A_{1630}) \times 100\%$ (1)

Nuclear magnetic resonance (NMR) spectroscopy

20 mg of sample was dissolved in 600 μL of D_2O to replace exchangeable protons and freeze-dried three times. Next the sample was dissolved in 600 μL of D_2O, centrifuged and the supernatant was collected into nuclear magnetic tube (5 mm). Both of ^1H NMR and ^{13}C NMR were available using a nuclear magnetic resonance spectrometer (AVANCE NEO, Bruker, Germany) equipped with ultra-low temperature probe at 298 K with the

operating frequency of 600 MHz.

Measurement of enzymatic hydrolysis products

Size distribution of enzymatic oligosaccharides was determined by Gel PermeationChromatography. 2 mg of enzymatic oligosaccharides mixture was injected in 1 mL distilled water, and filtered through a 0.22 μm membrane. 50 μL of solution was injected into the waters 1525 (Binary HPLC Pump) coupled with SuperdexTM peptide 10/300 GL (GE Healthcare, USA) and refractive detector. 0.3 M NH_4HCO_3 was used as the isocratic elution solution with a 0.4 mL/min flow rate at 25°C.

Phenol-sulfuric acid method

The amount of carbohydrates was regularly determined by phenol-sulfuric acid method.[5] To select collections rapidly which contained sugar clearly, 40 μL solution of collection samples was added into 96-well plate. Next 20 μL of 6% phenol and 200 μL of concentrated sulfuric acid were also added sequentially into samples. The reaction mixture was incubated at room temperature for 15 min to allow full color development. Determining the absorbance at 490 nm using Ultraviolet spectrophotometer (Thermo Fisher, USA) after allowing the reaction to complete.

MS/MS Spectrometry

1 mg of preparative oligosaccharide was dissolved in 1 mL of deionized water, diluted to 0.1 mg/mL and filtered through a 0.22 μm membrane. The supernatant was then placed in a sample vial for injection. Negative ion mode was selected in AB TripleTOF 6600plus System (AB SCIEX, Framingham, USA). source voltage was -4.5 kV, and the source temperature was 550℃. The pressure of Gas 1 (Air) and Gas 2 (Air) were set to 55 psi while the pressure of Curtain Gas (N2) was set to 35 psi with ±5 ppm set for maximum error. For MS/MS acquisition mode, the parameters were list: Declustering potential (DP), 80 V; collision energy (CE), 40 V; ion releasedelay (IRD), 67; ion release width (IRW), 25. The IDA-based auto-MS2 was analyzed on the 8 most intense metabolite ions in a cycle of full scan (1 s). The scan range of m/z of precursor ion and product ion were set as 100-2000 Da and 50-2000 Da. The exact mass calibration was performed automatically before each analysis employing the Automated Calibration Delivery System.

Fabrication of nanopipettes

The Quartz capillaries were first sequentially ultrasonic cleaned with isopropanol, ethanol, and deionized water for 30 mins each and then dried using nitrogen gas. The conical nanopipettes were fabricated using a CO_2 laser puller (P-2000, Sutter Instrument Co., California, USA) with those quartz glass capillaries. All the nanopipettes that had been pulled were cleaned using a Tergeo plasma cleaner (Tergo, California, USA) to clean the surfaces and make them more hydrophilic. All the nanopipettes used in the experiments were pulled using a two-step method.

(1) HEAT = 680, FIL = 4, VEL = 25, DEL = 160, PULL = 100

(2) HEAT = 680, FIL = 3, VEL = 15, DEL = 120, PULL = 180

The *I-V* curves of the nanopipettes in 1 M KCl solution were also taken to rough estimate the diameter following Eq. (2).[6]

$$d_i = \frac{4Gl}{\pi g d_b} \quad (2)$$

where d_i is the diameter of nanopipettes, G is the conductance of nanopipettes, l is the length of conical part of nanopipettes, g is the conductance of the solution, d_b is the diameter of the quartz capillary before pulling by CO_2 laser. The slope of the *I-V* curve refers to the nanopipette conductance. The obtained conductivity (G :

1.378x10^{-8} S), the length of conical nanopipettes (*l*: 4.2 mm), the conductivity of the 1M KCl solution (*g*: 11.18 S·m^{-1}; 25℃), and the capillary inner diameter before pulling (d_b: 0.5 mm) were substituted into the formula, which yielded a nanopipette diameter of approximately 13.2 nm.

Characterization of nanopipettes by TEM

A small piece of double-sided tape was attached to the edge of a 50×50 mesh double-layer copper grid (Beijing XXBR Technogy CO.,Ltd, China). A nanopipette was then carefully positioned with its tip on the copper grid, where it was supported by the double-sided tape. The position of the tip was adjusted slowly to ensure it was not obstructed by the copper grid. Once the tip's position was confirmed, a blade was used to gently press down on the cutting area to secure the tip to the double-sided tape. The cut nanopipette was examined under a microscope to verify that the tip was intact and clearly visible. After placing a lid over the copper grid, the tip was rechecked to ensure it remained complete. With the sample preparation complete, the prepared sample was then placed into the TEM for examination.

Nanopipette experimental procedures

Nanopipette experiments were conducted using an Axopatch 200B patch-clamp amplifier, which was coupled with a Digidata 1550B A/D converter (Molecular Devices, California, USA). Data acquisition was performed with Clampfit 10.7 software (Molecular Devices, California, USA) at a sampling rate of 100 kHz and a Bessel filter set to 10 kHz. The current preamplifier was interfaced with the patch-clamp amplifier. Ag/AgCl electrodes were inserted both inside and outside the nanopipette, with the external electrode grounded according to established protocols. Voltage was applied via a pair of Ag/AgCl electrodes. The open-circuit current was measured across a voltage range from -1000 mV to +1000 mV in a 1 M KCl solution to obtain *I*-*V* curves for the characterization of the bare nanopipettes.[7] Current traces were recorded under both positive voltages. Unless otherwise stated, all experiments were conducted in a phosphate-buffered solution (0.2 M, pH 7.4) containing 200 pM glycerol at 23 ± 2°C. All the raw current traces were low-pass filtered at 3 kHz for presentation.

Statistical Analysis

In nanopipette analysis, current signals events were extracted for dwell time and Δ*I* using the custom-designed PyNanoLab14.[8] All samples were processed with the “singleStepOriginal” mode. The signals with Δ*I* < 5 or dwell time < 0.1 ms were ignored. Multiple peak fitting was conducted for Δ*G* (Δ*I*/V) histograms (n > 1), and scatter plots of dwell time versus Δ*G* were generated using OriginLab software (OriginLab Corporation, Massachusetts, USA, https://www.originlab.com). All schematics and figure drawings were produced using Adobe Illustrator. The separation ratio (S) between two analytes was calculated following Eq. (3).[9]

$$S = |P_1 - P_2| / (W_1 + W_2) \quad (3)$$

where P_1 and P_2 represent the peak positions obtained from Gaussian fitting for each analyte, and W_1 and W_2 denote their corresponding full widths at half maximum (FWHM). The errors denote the standard deviation from at least three measurements unless noted otherwise.

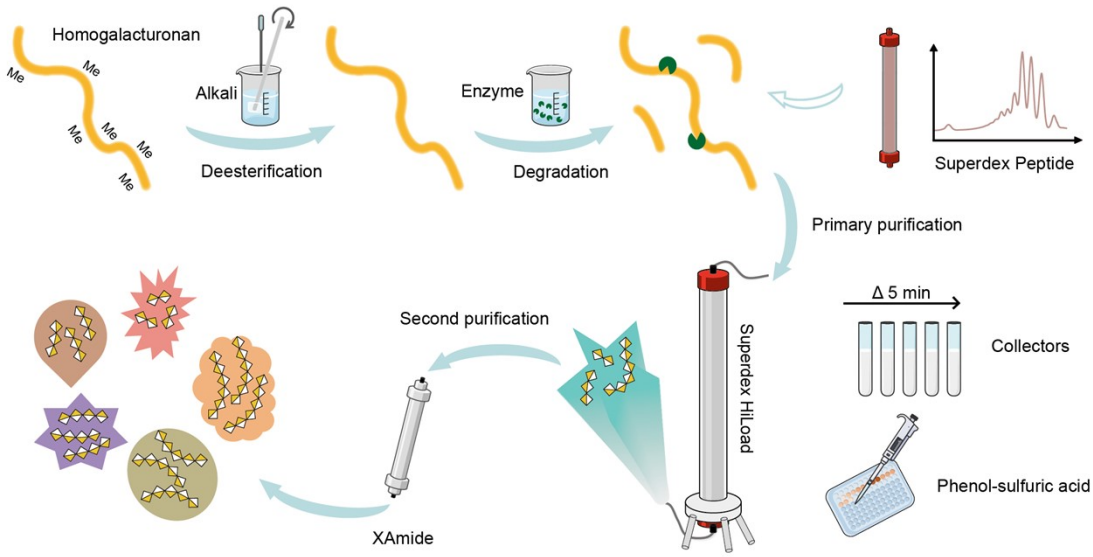

Figure S1. The detail schematic workflow of enzymatically hydrolyzed oligosaccharides preparation. After demethylesterification process by alkali, homogalacturonan was hydrolyzed into oligosaccharides products using Endo-Polygalacturonanase supporting with Superdex peptide. For primary purification, the products were separated into several collectors by Superdex HiLoad. The cubes containing oligosaccharides fragments were available with the detection by Phenol-sulfuric acid. Then the oligosaccharides mixtures were completely separated using preparative liquid chromatography (HILIC) equipped with XAmide column, obtaining pure GalA2-6 standards.

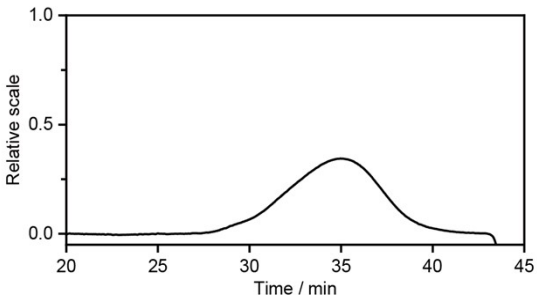

Figure S2. Size exclusion chromatogram profiles of demethylesterified polygalacturonic acid. The M_w, M_n of polysaccharide peak were calculated on ASTRA software.

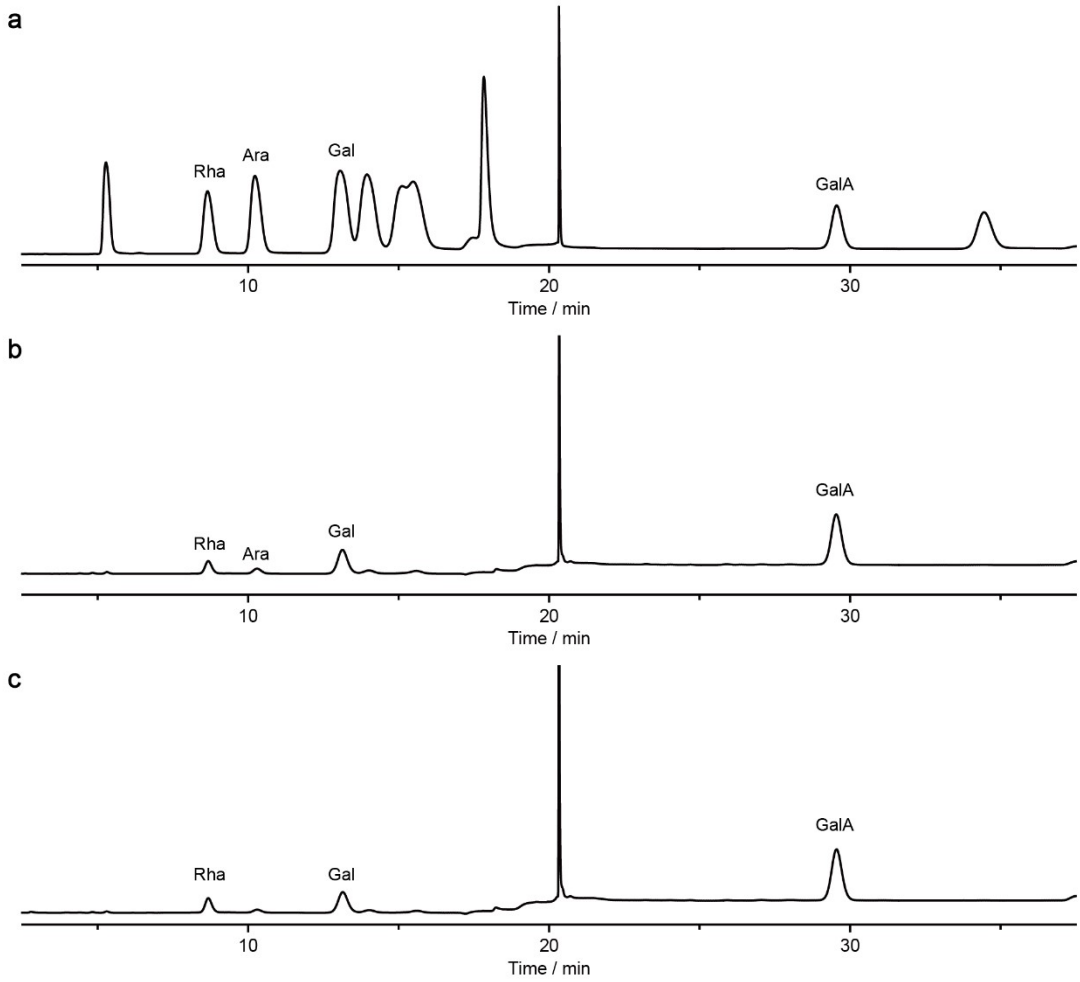

Figure S3. The monosaccharide chromatograms based on high-performance anion exchange chromatography of monosaccharide standards, polygalacturonic acid and demethylesterified polygalacturonic acid. (a) ten monosaccharide mixture standards in 100 μM (Fucose; Rhamnose; Arabinose; Galactose; Glucose; Mannose; Xylose; Ribose; Galacturonic acid; Glucuronic acid). (b) polygalacturonic acid, (c) demethylesterified polygalacturonic acid.

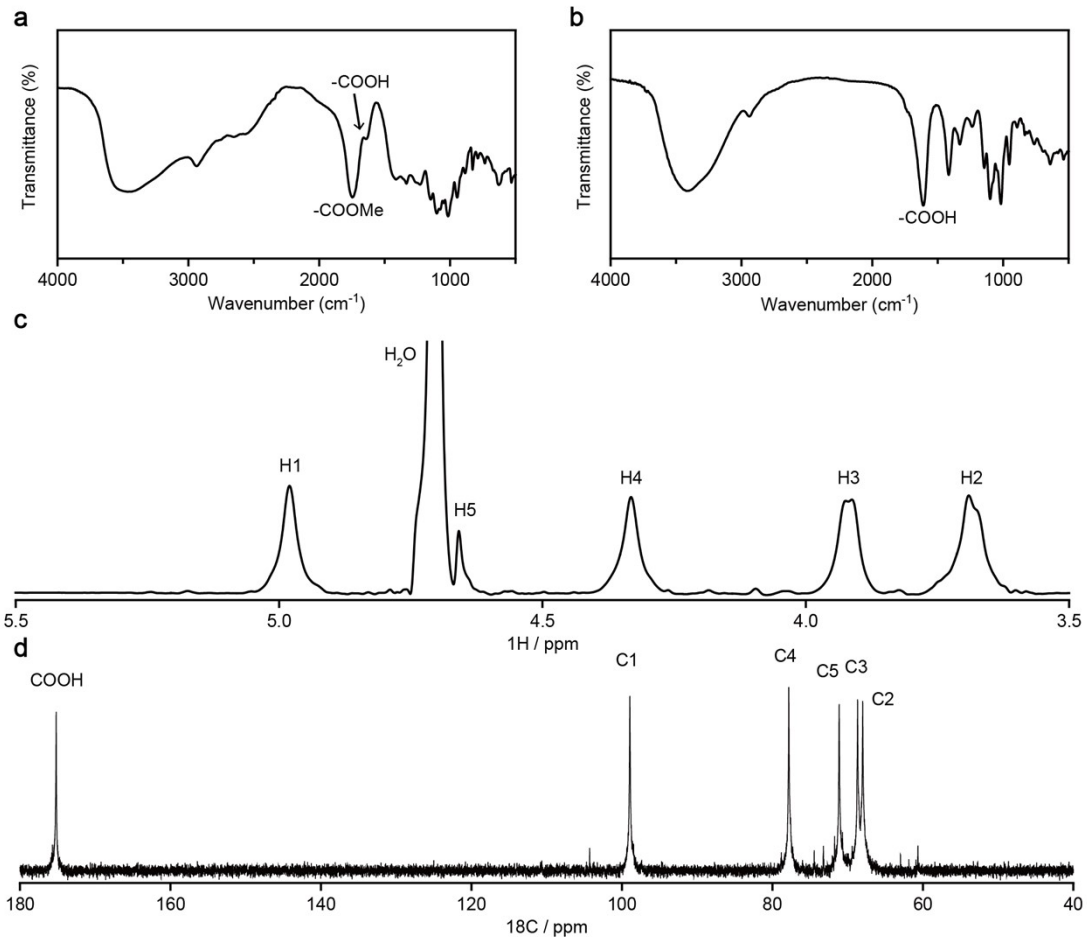

Figure S4. Structural characteristics of demethylesterified polygalacturonic acid. Infrared spectroscopy of polygalacturonic acid, demethylesterified polygalacturonic acid peaks at 1740 and 1630 cm^{-1} separately corresponded to the C=O stretching vibration of the methylesterificated carboxylic groups (COO−R) and asymmetric stretching of the carboxylate anions (COO−). The huge peak of COO−Me in polygalacturonic acid (a) indicated high degree of methylesterification. After the process of totally demethylesterification (b), the peak of COO−Me in demethylesterified polygalacturonic acid was disappeared. (c) 1H NMR spectrum of demethylesterified polygalacturonic acid. The chemical shift was referenced to the H_2O peak (δ = 4.79 ppm). All signal peaks of GalA (H1/5.07 ppm; H2/3.76 ppm; H3/4.01 ppm; H4/4.42 ppm; H5/4.75 ppm) were recorded in the spectra without characteristic peak of -OMe (δ = 3.84 ppm). (d) ^{13}C NMR spectra of demethylesterified polygalacturonic acid. All carbons signal peaks of GalA (C1/98.95 ppm; C2/68.00 ppm; C3/68.68 ppm; C4/77.82 ppm; C5/71.13 ppm; C6-COOH/175.20 ppm) were identified. The absence of peaks owing to C6-COOMe (δ = 170.72 ppm) and -OMe (δ = 52.83 ppm) also proved the success of demethylesterification.

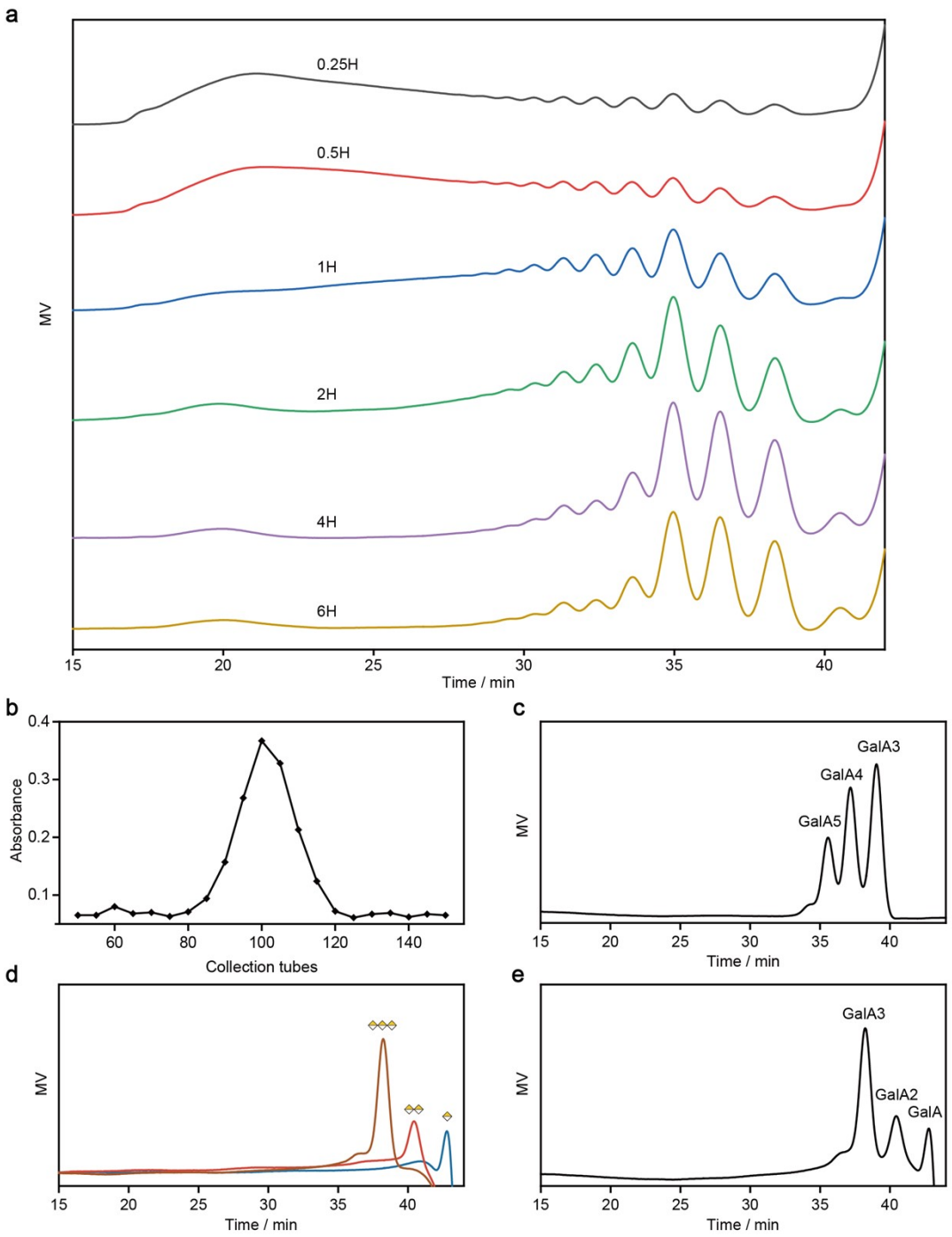

Figure S5. Preparation and crude collection of enzymatically hydrolyzed oligosaccharides. (a) Size distribution chromatograms of oligosaccharides mixtures at various enzymatic hydrolysis time (0.25 h, 0.5 h, 1 h, 2 h, 4 h, 6 h). As the reaction time increases, the degree of enzymatic hydrolysis continuously increases leading to lower degrees of oligosaccharides. Selection of a four-hours enzymatic hydrolysis time was based on the observation that the reaction approaches equilibrium generating optimal degrees of oligosaccharides. (b) Selection of crude oligosaccharides in collection tubes. The absorbance peak obtained from the sulfuric acid phenol confirms the presence of oligosaccharides in collection tubes 85-115. (c) Size distribution chromatograms of collection tube 100 provided the rough size of oligosaccharides with higher purity compared to Enzymatic hydrolysis mixture. (d) Size distribution chromatograms of individual oligosaccharides commercial standards (GalA, GalA2, GalA3) at 1mg/mL. (e) Size distribution chromatograms of oligosaccharides commercial standards mixtures (GalA1-3).

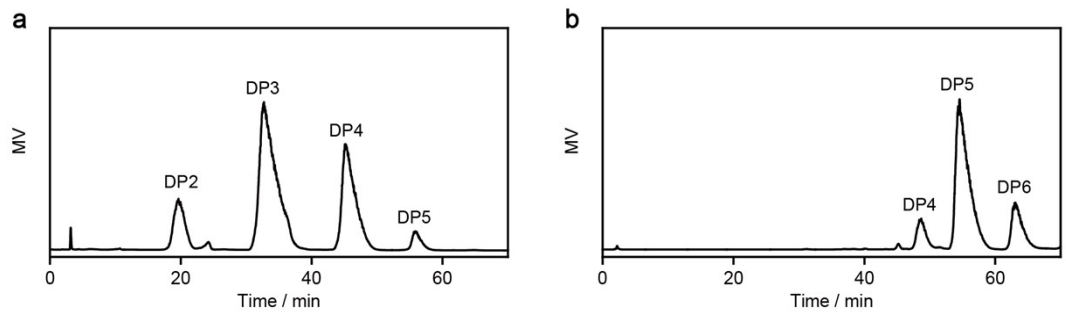

Figure S6. Preparative HILIC chromatograms for separation of crude oligosaccharides. Individual pure sample in DP2-5 (a) and DP4-6 (b) were obtained from two collection tubes.

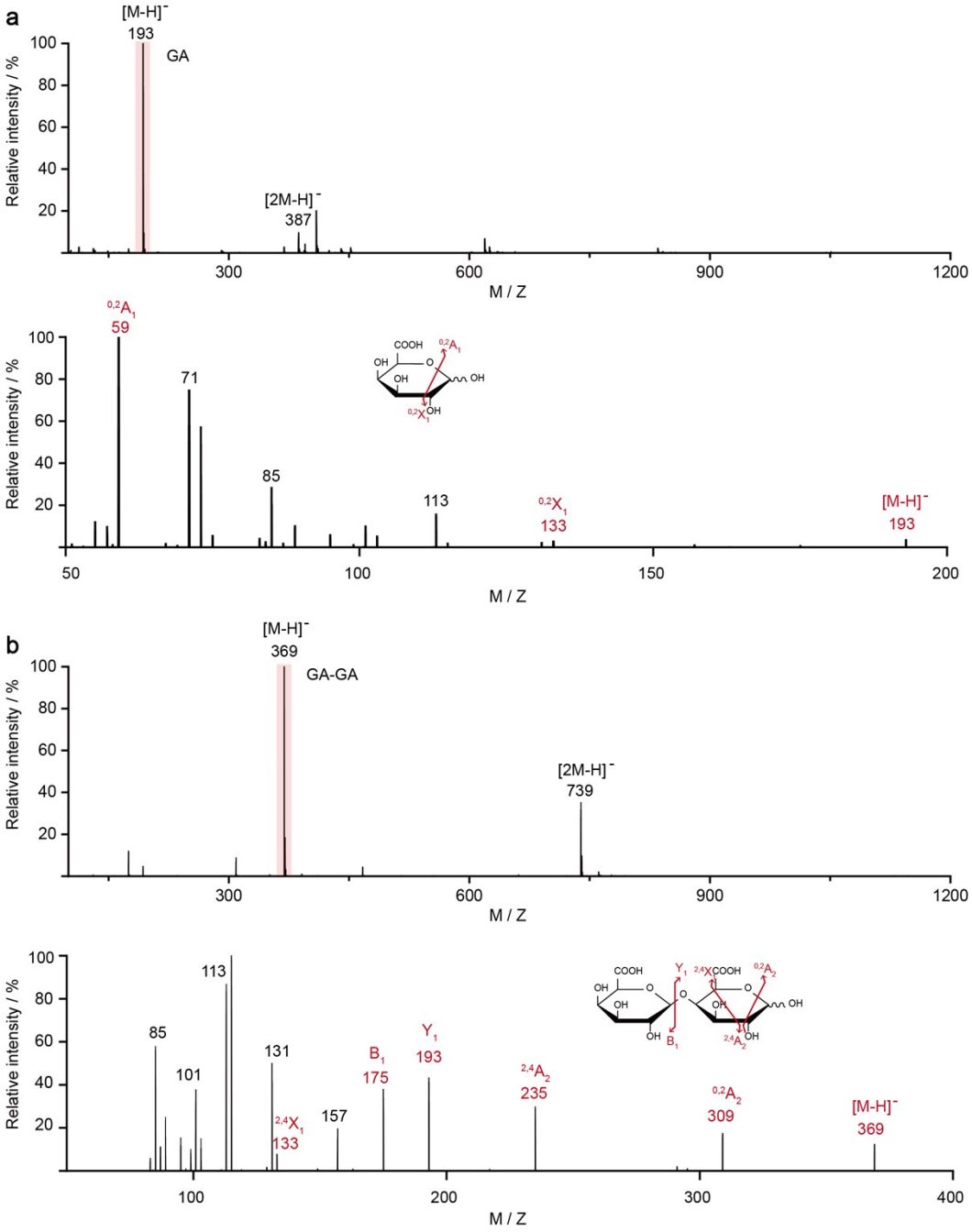

Figure S7. MS/MS spectra of GalA1-2 samples. The m/z at 193 (a), 369 (b) sequentially correspond to GalA and GalA2 with the secondary fragments of the parent ions presented.

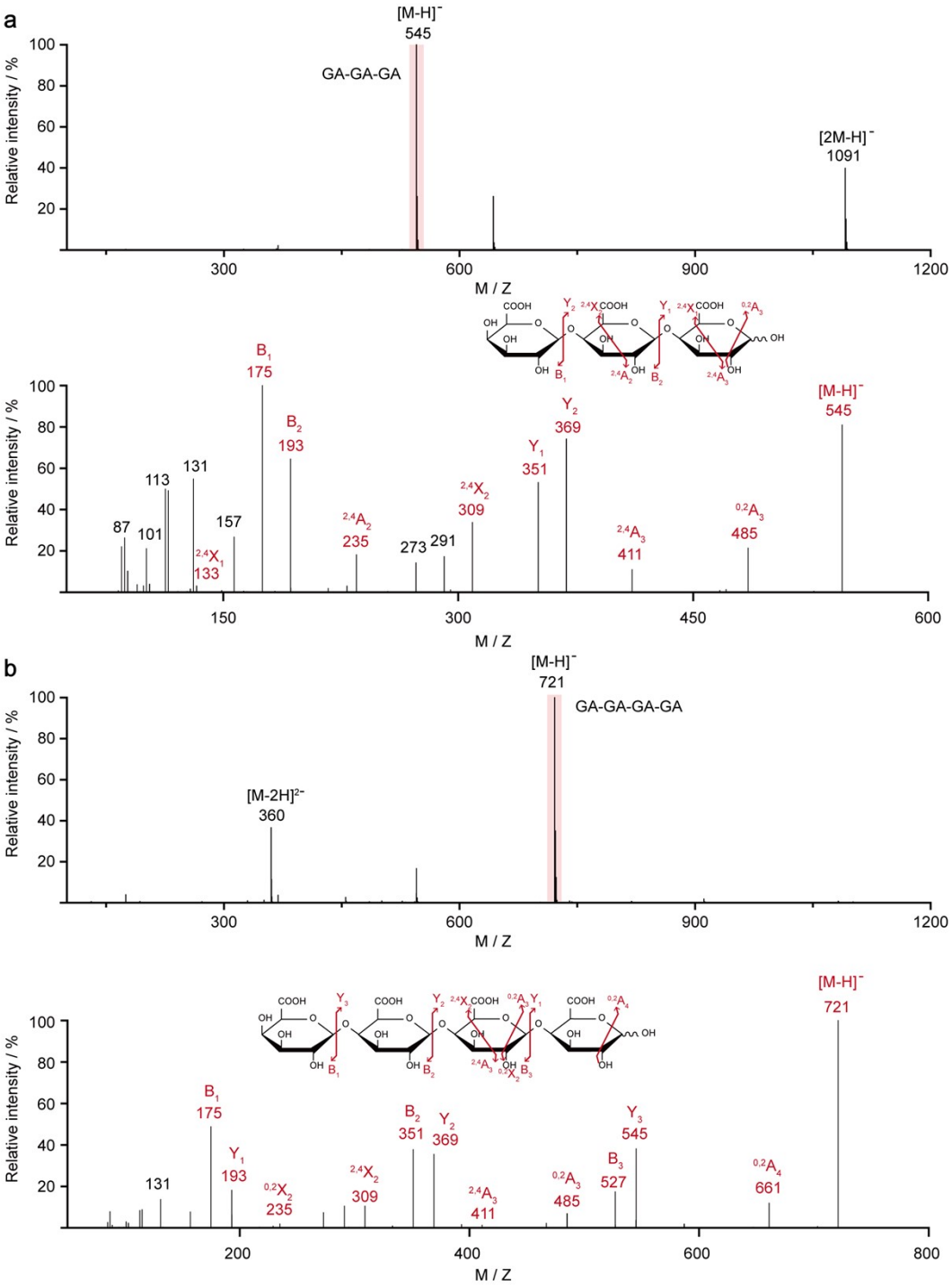

Figure S8. MS/MS spectra of GalA3-4 samples. The m/z at 545 (a), 721 (b) sequentially correspond to GalA3 and GalA4 with the secondary fragments of the parent ions presented.

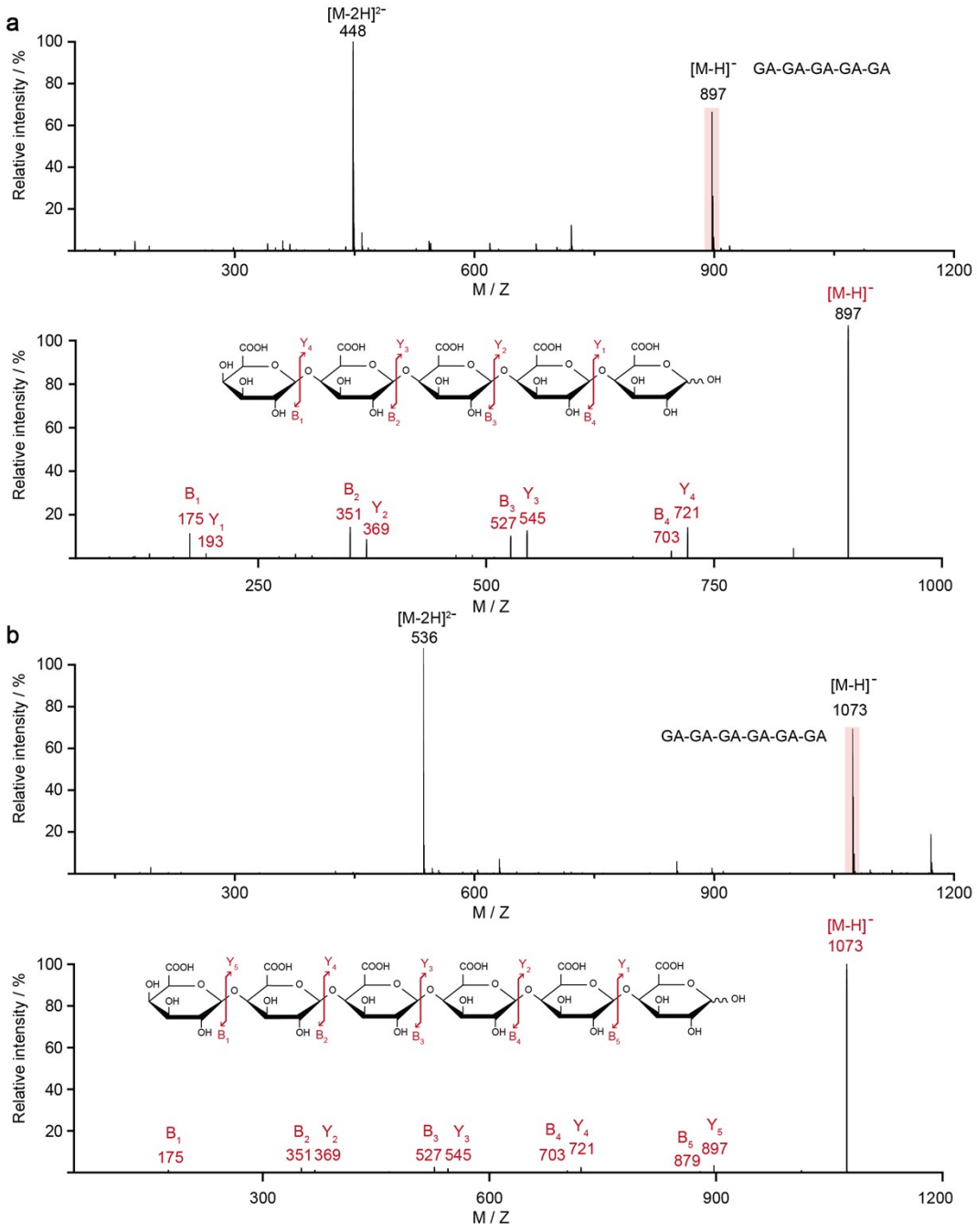

Figure S9. MS/MS spectra of GalA5-6 samples. The m/z at 897 (a), 1073 (b) sequentially correspond to GalA5 and GalA6 with the secondary fragments of the parent ions.

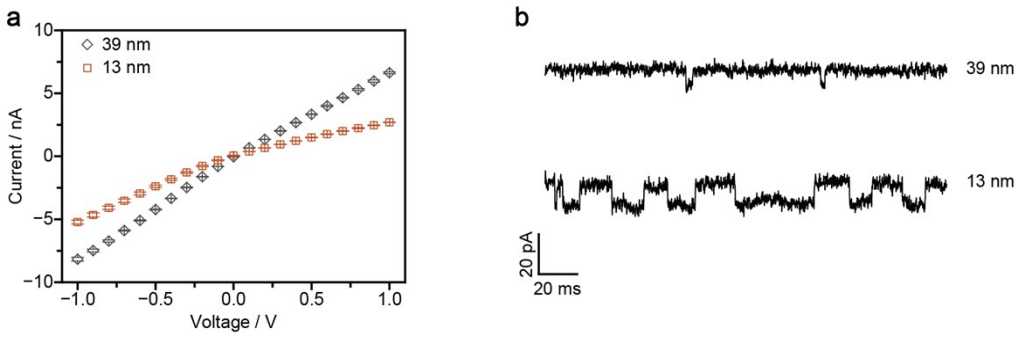

Figure S10. The signals of GalA5 sensing from nanopipettes in varying diameters. *I-V* curves (a) of nanopipettes with 39 nm and 13 nm diameters, measured in 0.2 M PB (pH = 7.4) containing 200 pM glycerol. The smaller blockage signals and shorter dwell time were clear in nanopipettes with 39 nm diameter (b) in 0.2 M PB solution at pH = 7.4 under the applied voltage of 600 mV.

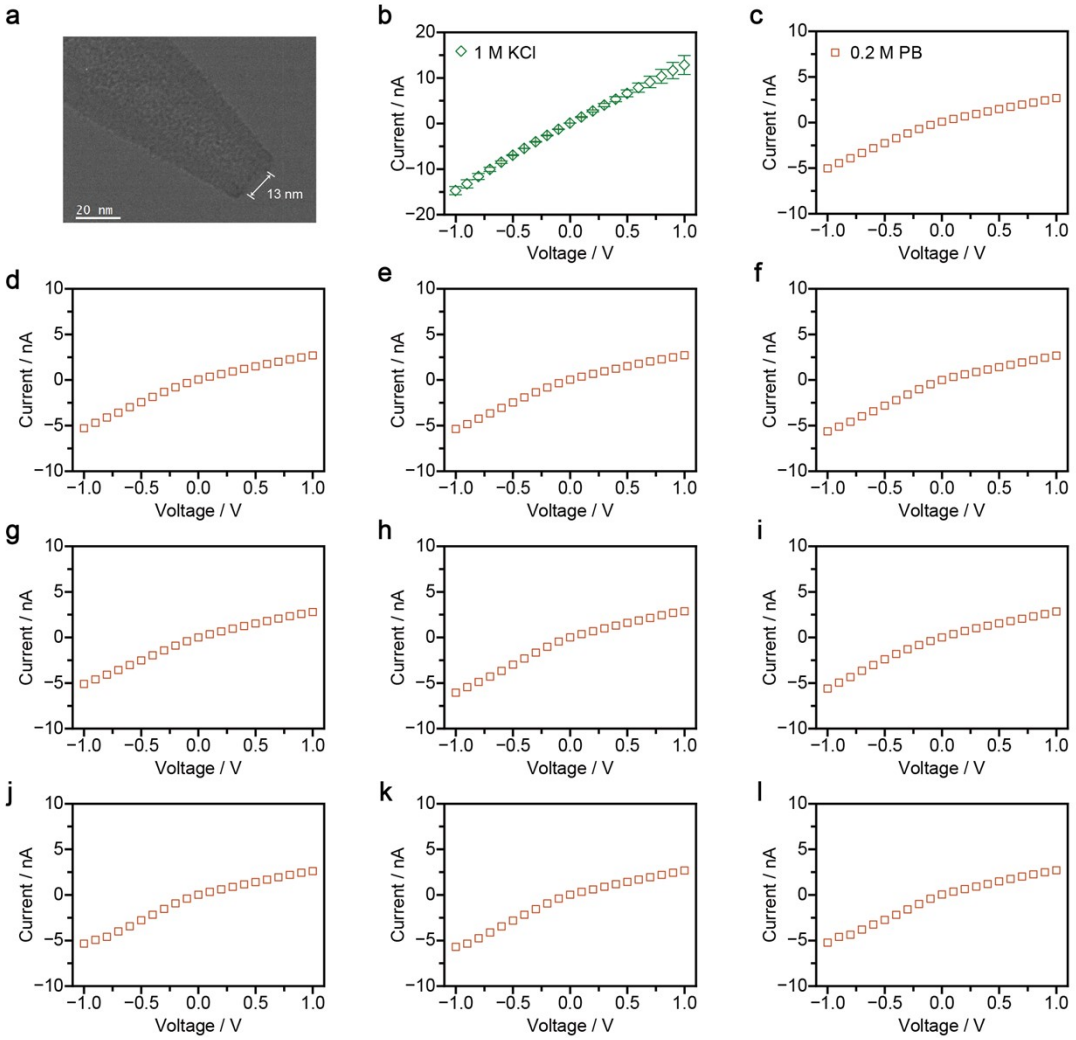

Figure S11. Characterization of nanopipettes and stability. (a) TEM image of a nanopipette with a 13 nm diameter. (b) Current-voltage (*I*-*V*) curves of nanopipettes, measured in 1 M KCl solution. The errors denote the standard deviation from at least three independent experiments. (c-l) *I*-*V* curves of nanopipette, measured in 0.2 M PB (pH = 7.4) containing 200 pM glycerol.

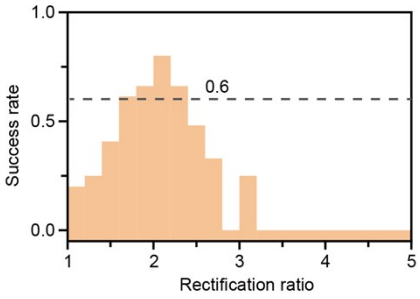

Figure S12. Optimal rectification ratio range of nanopipettes for single-molecule detection of galacturonic acid oligosaccharides. The success rate is an defined as event Frequency ＞ 0.1 s^{-1} and a signal-to-noise ratio (SNR)＞ 3. The rectification ratio is calculated as $|I_{-600}$ mV / I_{+600} mV|. An optimal rectification ratio range of 1.6–2.4 is identified, within which the success rate exceeds 0.6. All experiments were performed in 0.2 M phosphate buffer (PB, pH 7.4) with trace amounts of glycerol. The results from 61 independent experiments.

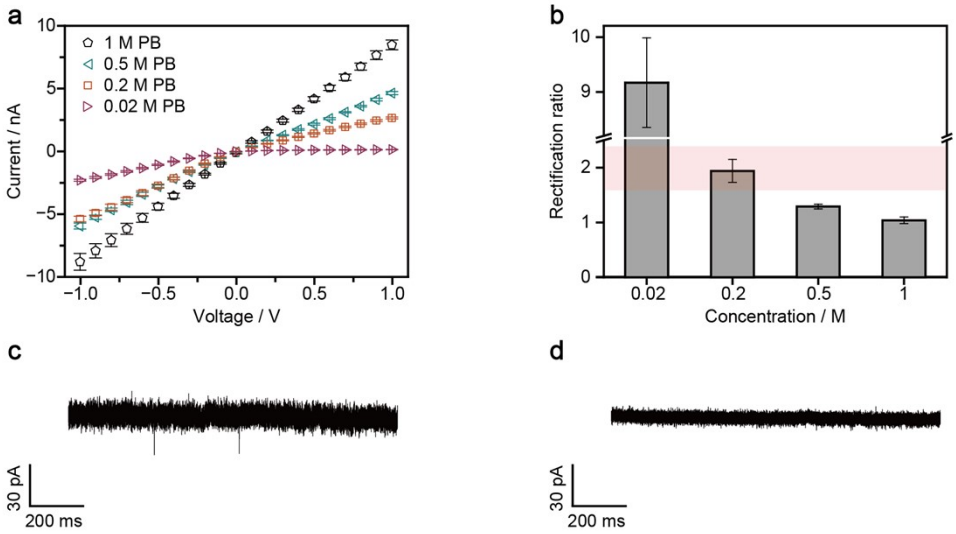

Figure S13. Solution concentration dependence of the current rectification. (a) *I-V* curves of nanopipettes in concentration of PB solution from 0.02 M to 1 M containing 200 pM glycerol at pH = 7.4. The rectification ratios (b) of corresponding concentrations of PB solution were provided, only rectification ratios of 0.2 M PB fell within the optimal rectification ratio range highlighted with a pink rectangle (1.6-2.4). (c) The row current trace of GalA6 measured using nanopipettes in 1 M PB solution at pH = 7.4 under the applied voltage of 600 mV, recording the scant signals with extremely short dwell time. (d) No signals were observed for GalA6 in 0.02 M PB under the applied voltage of 600 mV. The errors denote the standard deviation from at least three independent experiments.

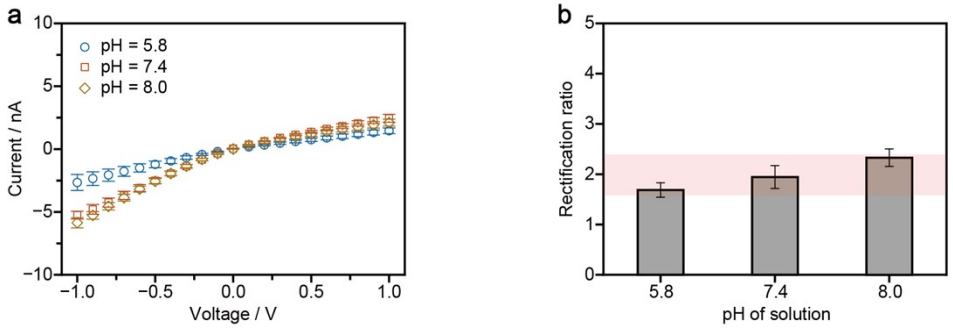

Figure S14. pH dependence of the current rectification. (a) I-V curves of nanopipettes in hydrogen ion concentration of 0.2 M PB solution containing 200 pM glycerol from 5.8 to 8.0. (b) When pH of PB solution were 5.8 or 8.0, the rectification ratios were just near the boundary of optimal rectification ratio range. The errors denote the standard deviation from at least three independent experiments.

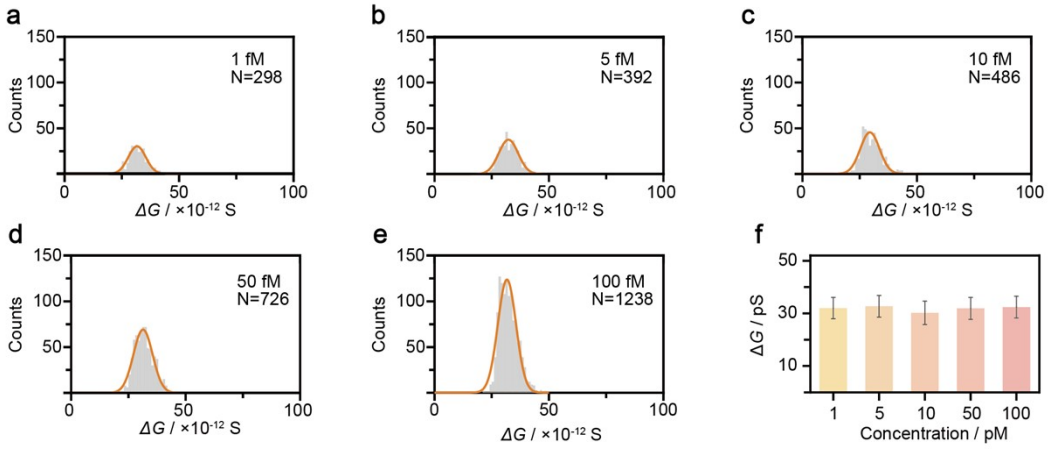

Figure S15. (a-e) Concentration-independent Δ*G* histograms of GalA6 from 1 fM to 100 fM (bin size = 1). (f) Mean Δ*G* with standard deviation across the concentration range. The error bars represent the half width at half maximum (HWHM).

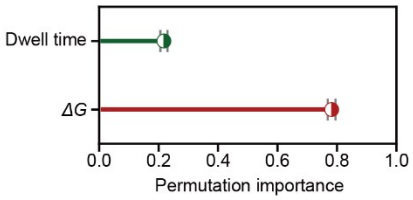

Figure S16. The feature importance of the random forest model**.** The conductivity feature contributed approximately 80% in making predictions.

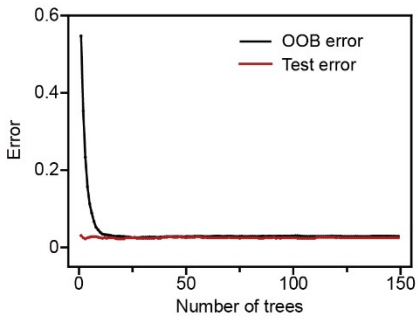

Figure S17. Iteration Diagram of the random forest model. The out-of-bag (OOB) error was an unbiased estimate of the generalization error of the random forest model, and it was established during the generation process without cross-validation. The OOB error and test error were gradually declining with increasing number of trees and reached convergence when the number of trees exceeded 20.

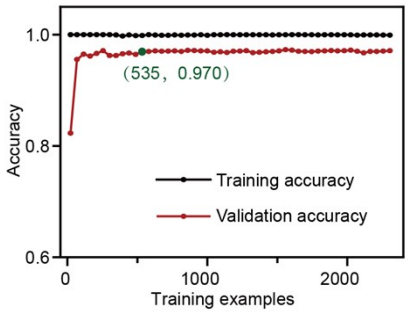

Figure S18. Learning curve of the Random Forest model. The validation accuracy increased with the number of training samples and stabilized at approximately 0.970 when the training set exceeded 535 samples, indicating strong generalization ability.

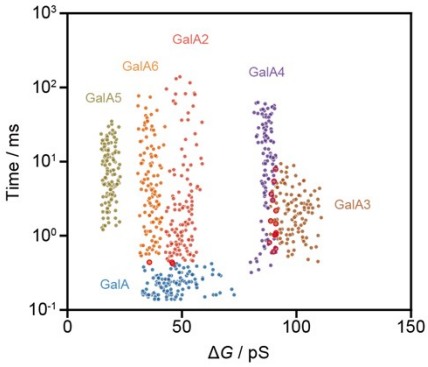

Figure S19. Scatter plot of predicted test data using the Random Forest model. Different oligosaccharides were color-coded according to their classification results, with misclassified events highlighted by red circles.

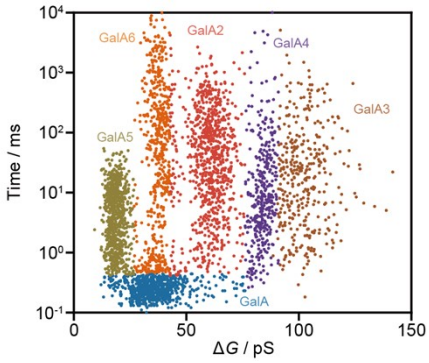

Figure S20. Scatter plot of predicted data from the mixture containing six oligosaccharides using the Random Forest model**.** Different oligosaccharides were color-coded according to their classification results.

Table S1. Average values of molecular weight of demethylesterified polygalacturonic acid.

	M_w[a] (kDa)	M_n[b] (kDa)	M_w/M_n[c]
HGTZ	75.68 (±1.108%)	30.67(±3.780%)	2.468 (±3.939%)

[a]M_w: Weight-average molecular weight.

[b]M_n: Number-average molecular weight.

[c]M_w/M_n: represents polydispersity.

Table S2. Monosaccharide Composition (mol%) of polysaccharides.

	Monosaccharide Composition (mol%)			
	Rha	Ara	Gal	GalA
HG	6.38	2.60	11.83	79.19
	±0.15	±0.03	±0.37	±0.54
HGTZ	7.55	/	9.89	82.55
	±0.33		±0.05	±0.39

Rha: rhamnose, Ara: arabinose, Gal: galactose, GalA: galacturonic acid.

Table S3. The ratio of success number to total number across different range in rectification ratio of nanopipettes.

Rectification ratio	Success number/Total number	Rectification ratio	Success number/Total number
1.00-1.19	1/5	3.00-3.19	1/4
1.20-1.39	2/8	3.20-3.39	0/1
1.40-1.59	3/7	3.40-3.59	0/0
1.60-1.79	5/8	3.60-3.79	0/1
1.80-1.99	2/3	3.80-3.99	0/1
2.00-2.19	8/10	4.00-4.19	0/1
2.20-2.39	2/3	4.20-4.39	0/1
2.40-2.59	1/2	4.40-4.59	0/1
2.60-2.79	1/3	4.60-4.79	0/1
2.80-2.99	0/1	4.80-4.99	0/0

Table S4. Comparison of this work and other nanopores for glycan profiling.

Nanopore	Analyte	Detection limit	journal
Biological nanopores	Monosaccharide	20 mM	*Angew Chem Int Ed.* 2022, 61
	Neutral glycans(dp2-4)	20 μM	*ACS Nano* 2024, 18, 12412
	LacNAc-series glycans(dp2-10)	100 μM	*J. Am. Chem. Soc.* 2025, 147, 1721
SiN_x nanopores	Monosaccharide	3 μM	*Sci Rep.* 2024, 14, 32000
Nanopipette	trisaccharide	10 μM	*Nano Lett.* 2024, 24, 5639
	galacturonic acid oligosaccharides(dp1-6)	1 fM	This work

Reference

1 P. J. H. Daas, A. G. J. Voragen and H. A. Schols, *Biopolymers*, 2001, **58**, 195–203.

2 W. Liang, J. Liao, J.R. Qi, W. Jiang and X. Yang, *Food Chem.*, 2022, **375**, 131806.

3 K. Zhu, J. Wu, A. Hu, Z. Yin, Z. Hou, X. Ye and S. Chen, *J. Agric. Food Chem.*, 2024, **72**, 9117–9127.

4 P. Zhao, X. Li, Y. Wang, L. Yan, L. Guo, L. Huang and W. Gao, *Carbohydr. Polym.*, 2020, **233**, 115836.

5 J. Wu, K. Zhu, J. Li, X. Ye and S. Chen, *Int. J. Biol. Macromol.*, 2024, **277**, 133591.

6 R. Gao, Y.L. Ying, B.Y. Yan, P. Iqbal, J. A. Preece and X. Wu, *Microchim Acta*, 2016, **183**, 491–495.

7 H. Ma, R.J. Yu, Y.L. Ying and Y.T. Long, *J. Electroanal. Chem.*, 2022, **908**, 116086.

8 S.C. Liu and Y.T. Long, *Zenodo*, DOI:10.5281/zenodo.11383973.

9 G. Yao, Y. Tian, W. Ke, J. Fang, S. Ma, T. Li, X. Cheng, B. Xia, L. Wen and Z. Gao, *J. Am. Chem. Soc.*, 2024, **146**, 13356–13366.